

# Multiband Antenna for GPS, IRNSS, Sub-6 GHz 5G and WLAN Applications

Devendra H. Patel<sup>1, 2, \*</sup> and Gautam D. Makwana<sup>3, \*</sup>

**Abstract**—An elliptical shape multi-band microstrip patch antenna with narrow semicircle cuts and bulges on two horizontal ends is proposed for Global Positioning System (GPS), Indian Regional Navigation Satellite System (IRNSS), Sub-6 GHz 5G and Wireless Local-Area Network (WLAN) wireless communication applications. The proposed antenna operates at 1.56 GHz, 2.49 GHz, 3.5 GHz, and 5.24 GHz for desired applications, respectively. The proposed antenna, fed by coaxial feeding mounted on Rogers AD255C substrate, has optimized physical dimensions of  $80 \times 80 \times 3.175 \text{ mm}^3$ . The semicircle cuts and bulges on horizontal ends on the elliptical element contribute to exciting higher-order modes and affect the current distribution at the resonant frequencies resulting in producing multi-band operations. The proposed antenna is fabricated and tested. The measured return loss characteristic ( $S_{11}$ ) below  $-10 \text{ dB}$  is  $-15.2 \text{ dB}$ ,  $-19 \text{ dB}$ ,  $-22.3 \text{ dB}$ , &  $-27.9 \text{ dB}$ , with the radiation efficiency of 58.7%, 94.8%, 93.2%, & 84.9% and peak gain of 3.49 dBi, 6.49 dBi, 4.93 dBi, & 4.46 dBi for desired application band, respectively. The proposed antenna also offers impedance bandwidths of 40 MHz (1.55–1.59 GHz), 90 MHz (2.43–2.52 GHz), 100 MHz (3.44–3.54 GHz), & 90 MHz (5.23–5.32 GHz) at resonant frequencies and relatively stable radiation patterns. Simulated and measured results for the proposed antenna exhibit good agreement. The proposed multi-band antenna offers a simple design and improved performance.

## 1. INTRODUCTION

A necessity for multi-band antennas covering many applications frequency bands such as cellular communications network/generation, Second Generation (2G), Third Generation (3G), Fourth Generation (4G), Fifth Generation (5G), IRNSS, GPS, Wireless Fidelity (Wi-Fi), and Worldwide Interoperability for Microwave Access (WiMAX), at once is currently in the demand for wireless communication systems because they can reduce the number of antennas required. It is difficult to design an effective multi-band antenna that can function effectively in multiple assigned frequency bands offering a simple design, compact size, easy manufacturing, simplicity of integration with other circuit elements and feed networks, etc. [1–3]. Recently, there has been a lot of research on traditional microstrip antenna designs/geometries including slots, fractals, split ring resonators (SRRs), reconfigurable frequency, parasitic elements, etc. operating at multi-resonant frequencies sought in many real-world applications including navigation, mobile, radar, and other wireless communication systems [1–3]. Researchers and designers are nowadays working on novel multi-band antennas that offer a simple design, low complexity, small size, suitable impedance bandwidth, radiation patterns, gain, radiation efficiency, directivity, etc. [1–3]. However, designing a structure for multi-band operations

---

*Received 9 February 2023, Accepted 21 March 2023, Scheduled 3 April 2023*

\* Corresponding authors: Devendra H. Patel (pateldevendrah@gmail.com), Gautam Durlabhji Makwana (gmakwana@gmail.com).

<sup>1</sup> Sankalchand Patel University, Visnagar, India. <sup>2</sup> Electronics & Communication Engineering Department, Government Engineering College, Gandhinagar, India. <sup>3</sup> Electronics & Communication Engineering Department, GTU — Graduate School of Engineering and Technology, Gujarat Technological University, Ahmedabad, India.

that offers a low-profile design and like performance in each band is still challenging for researchers. Several methods have currently been reported for the design of multi-band antennas [3–6].

One of the most effective wireless systems is a satellite-based navigation system. The U.S. government maintains the control of GPS, a well-known satellite-based navigation system. Several other nations, including India, Russia, EU, China, and Japan, have also launched their navigation satellite systems, IRNSS, GLONASS, Galileo, BeDou, and QZSS, respectively. The Indian Space Research Organization (ISRO)-India has also developed a new space-based positioning and navigational system known as IRNSS which operates at 1176.45 MHz & 2492.028 MHz in the L5 & S-band, respectively [7]. For satellite, cellular networks, defence, military, and civilian purposes, numerous researchers, engineers, and organizations are developing multi-band antennas that accommodate GPS, IRNSS, and other wireless communication applications. Mandal and Pattnaik [8] reported a coplanar waveguide (CPW)-fed multi-band wearable monopole antenna to cover the 1.8 GHz, 2.4 GHz/5.2 GHz, & 3.5 GHz for Global System for Mobile Communications (GSM), WLAN, & WiMAX bands, respectively by creating slanted monopoles of various lengths from an isosceles triangular patch. Kwon et al. [9] reported a three-dimensional compact shark-fin antenna covering 0.850 GHz, 1.575 GHz, 2.4 GHz, and 5.9 GHz for MIMO-LTE, GPS, WLAN, and Wireless Access in the Vehicular Environment (WAVE) bands, respectively. Naik et al. [10] demonstrated a spiral-based antenna for GPS and IRNSS. Modi et al. [11] reported a compact multi-band wide-band antenna for IRNSS, 4G, 5G, and satellite applications. The literature review shows that many intriguing and cutting-edge ideas have been recently explored to create multi-band microstrip antenna structures with linear polarization, bandwidth, and pattern changeable characteristics. It is also realized that multi-band microstrip patch antennas are usually designed using common patch shapes, rectangle, triangle, square, annular-ring, etc. However, it is possible to attain an electrically small-size multi-band microstrip patch antenna without compromising radiation performance if the shape is made circular or elliptical compared to other patch shapes [1, 2, 12]. Trzaska [22, 23] reported methods for measuring Electromagnetic Field (EMF) in the near-field and far-field. In line with this, it was tried to accommodate satellite-based navigation systems GPS and IRNSS along with WLAN and Sub-6 GHz 5G wireless applications in view of an Indian navigation system.

The paper is organized as follows. Section 2 provides details of the design approach and configuration of the proposed antenna. Simulated and measured results are discussed in Section 3. Lastly, the proposed antenna is summarized in a conclusion section.

## 2. ANTENNA DESIGN APPROACH AND CONFIGURATION

### 2.1. Antenna Design Approach

A circular patch/disc antenna that serves as the foundation of the proposed antenna design can be properly analyzed using a cavity model. Radiating modes supported by the circular patch antenna can be determined by modeling the patch, a ground plane, and a separator medium as a substrate that form a circular cavity. The modes  $TM^z$  can be supported by a circular microstrip patch antenna with a relatively low substrate height,  $h$ , (i.e.,  $h < 0.05\lambda_0$ , where  $\lambda_0$  is a free-space wavelength) with almost constant fields along  $z$  (i.e.,  $z$  is taken perpendicular to the patch). A radius,  $a$ , of the circular patch can be used to control or vary the modes, changing the absolute resonance frequency of each mode without changing the order of the modes [1]. A vector potential method to locate the fields inside the cavity by determining the magnetic vector potential  $A_z$  as Equation (2) for the electric and magnetic field of  $TM^z$  mode must fulfill the homogeneous wave equation as Equation (1) [1]:

$$\nabla^2 A_z(\rho, \phi, z) + k^2 A_z(\rho, \phi, z) = 0 \quad (1)$$

$$A_z = B_{mnp} J_m(k_\rho \rho') [A_2 \cos(m\phi') + B_2 \sin(m\phi')] \cos(k_z z') \quad (2)$$

where,  $k_\rho = \chi'_{mn}/a$ ,  $k_z = p\pi/h$ ,  $m = 0, 1, 2, \dots$ ,  $n = 1, 2, 3, \dots$ ,  $p = 0, 1, 2, \dots$

The fields inside the cavity are represented by the primed cylindrical coordinates  $\rho'$ ,  $\phi'$ , and  $z'$ . Therefore, in the cavity model, Equations (3)–(6) are used to determine the resonant frequencies for the  $TM^z_{mn0}$  modes by considering  $p = 0$  &  $k_z = 0$  in constraint Equation (3) [1]. As a correction factor, while the fringing effect is taken into account, the actual radius ( $a$ ) is swapped out for an effective radius

( $a_{eff}$ ) as given in Equation (6) [1].

$$(k_\rho)^2 + (k_z)^2 = (k_r)^2 = \omega_r^2 \mu \epsilon \tag{3}$$

$$(f_r)_{mn0} = \frac{1}{2\pi\sqrt{\mu\epsilon}} \left( \frac{\chi'_{mn}}{a} \right) = \frac{\chi'_{mn} v_0}{2\pi a \sqrt{\epsilon_r}} \Rightarrow (f_{rc})_{mn0} = \frac{\chi'_{mn} v_0}{2\pi a_{eff} \sqrt{\epsilon_r}} \tag{4}$$

$$a = \frac{F}{\left\{ 1 + \frac{2h}{\pi\epsilon_r F} \left[ \ln \left( \frac{\pi F}{2h} \right) + 1.7726 \right] \right\}^{1/2}}, \quad F = \frac{8.791 \times 10^9}{f_r \sqrt{\epsilon_r}}, \quad h \text{ in cm} \tag{5}$$

$$a_{eff} = a \left\{ 1 + \frac{2h}{\pi a \epsilon_r} \left[ \ln \left( \frac{\pi a}{2h} \right) + 1.7726 \right] \right\}^{1/2} \tag{6}$$

where  $f_r$ : resonant frequency,  $a$ : actual radius of a circular patch,  $\epsilon_r$ : substrate dielectric constant,  $h$ : substrate height,  $a_{eff}$ : effective radius after considering a fringing effect,  $v_0$ : speed of light,  $\chi'_{mn}$ : zeroes of the Bessel function's ( $J_m(x)$ ) derivative with  $\chi'_{11} = 1.8412$ ,  $\chi'_{21} = 3.0542$ , and  $\chi'_{31} = 4.2012$  values to establish the order of the resonant frequencies.

A design process that results in functional designs of the proposed microstrip patch antenna starts with the excitation of dominating  $TM_{110}^z$  mode based on the cavity model formulation as described in Equations (1)–(6) [1]. The conventional circular patch antenna is used to produce the fundamental frequency of 5.208 GHz by exciting dominant mode  $TM_{11}$ . The second resonating frequency of 3.516 GHz is achieved by reshaping the antenna in an elliptical shape and by segregating the dominant mode  $TM_{11}$  into its orthogonal modes' components ( $TM_{11h}$  &  $TM_{11v}$ ) (i.e., by exciting orthogonal resonance modes). The third resonating frequency of 2.45 GHz is achieved by exciting one higher order mode  $TM_{21}$  along with orthogonal modes, by reshaping the antenna with an elliptical shape patch, and by introducing semicircle cuts & bulges on the patch. The fourth resonating frequency of 1.56 GHz is achieved by exciting two higher-order modes  $TM_{21}$  and  $TM_{31}$  with orthogonal modes simultaneously and by reshaping the antenna and changing the position of the feed, semicircle cuts & bulges, and patch. Other higher-order modes are adjusted in such a way that they will not resonate. Figure 1 shows a stepwise design of the proposed antenna geometry using the cavity model-circular patch theory. Step-1 shows single-band; Step-2 shows dual-band; Step-3 shows triple-band; and Step-4 shows quad/multi-band design evolution.

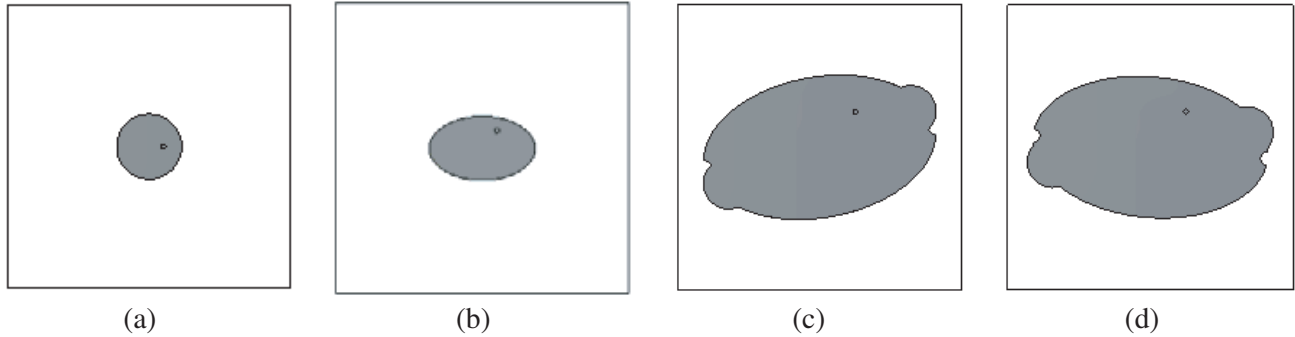


**Figure 1.** Stepwise design of the proposed antenna using cavity model-circular patch theory. (a) Step-1: Single-band (Radius: 9.2 mm, Frequency: 5.208 GHz). (b) Step-2: Dual-band (Radius: 14.5 mm & 8.8 mm, Frequency: 3.516 GHz & 5.202 GHz). (c) Step-3: Triple-band (Radius: 33 mm & 19.81 mm, Frequency: 2.45 GHz, 3.44 GHz & 5.23 GHz). (d) Step-4: Quad/Multi-band (Radius: 33 mm & 19.3 mm, Frequency: 1.56 GHz, 2.49 GHz, 3.5 GHz & 5.24 GHz).

### 3. ANTENNA CONFIGURATION

The proposed multi-band antenna consists of an elliptical shape patch with narrow semicircle cuts and bulges on two horizontal ends for GPS, IRNSS, Sub-6 GHz 5G, and WLAN wireless communications

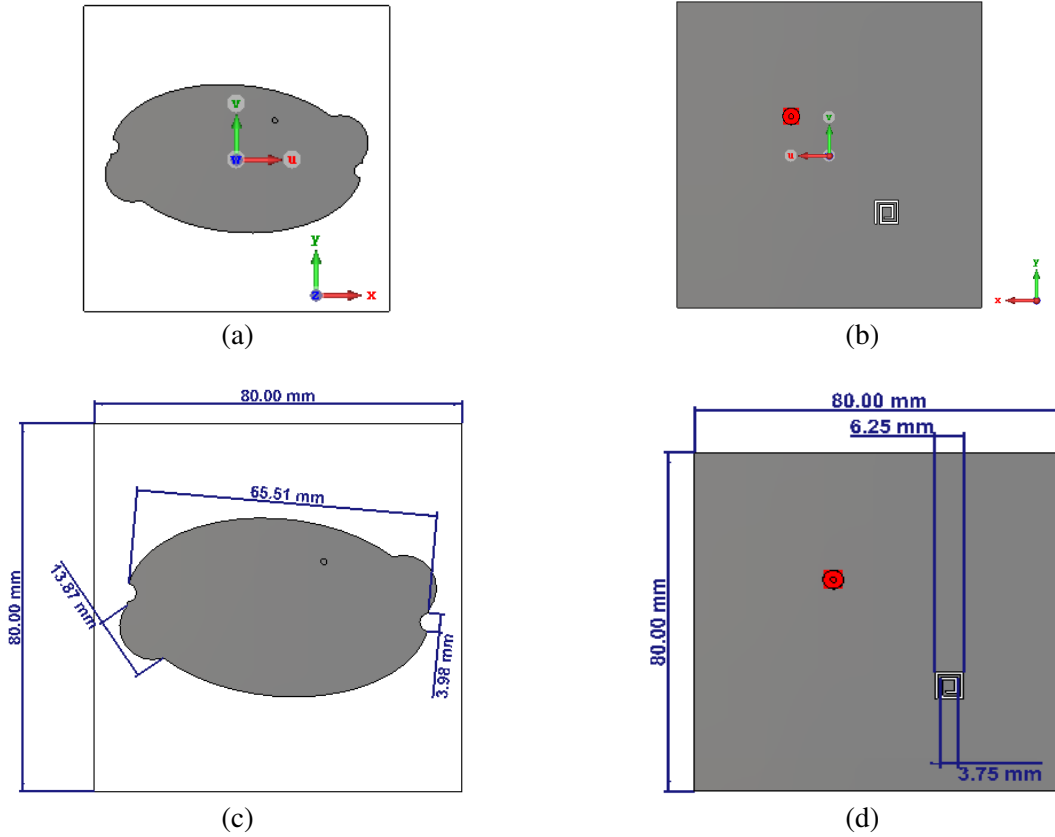


**Figure 2.** Proposed antenna design: (a)–(b) Top view & bottom view. (c)–(d) Top view & bottom view with dimensions.

applications as shown in Figure 2. The proposed antenna having dimensions of  $80 \times 80 \times 3.175 \text{ mm}^3$  is mounted on a Rogers AD255C substrate with a loss tangent ( $\tan \delta$ )  $< 0.002$  and relative permittivity ( $\epsilon_r$ ) of 2.6. The antenna is fed by a coaxial probe feeding at (10 mm, 10 mm) point. The antenna is optimized to get more appropriate resonance at 1.56 GHz, 2.49 GHz, 3.5 GHz, & 5.24 GHz for the desired application. A square spiral shape slot in the ground plane is introduced to remove undesired bands. The characteristics of the proposed antenna are simulated in CST Studio Suite 2020, and the measurement of the fabricated antenna is carried out in an anechoic chamber as shown in Figure 3.

In this study, measurements of the reflection coefficient, voltage standing wave ratio (VSWR), radiation patterns, gain, and efficiency of the proposed antenna are performed and compared with the simulated results.

#### 4. RESULTS AND DISCUSSION

CST Studio Suite 2020 has been used for the simulations of various parameters of the proposed antenna, and measurements of the fabricated antenna are made in an anechoic chamber using a vector network analyzer (VNA). The simulated reference impedance ( $z_{ref}$ ) of the reported antenna is  $48.55 \Omega$ .

The measured reflection coefficient ( $S_{11}$ ) and VSWR of the proposed antenna are shown in Figure 4(a) and Figure 4(b), respectively with the concerned simulated results. Figure 4 shows the measured results, and the simulated results accord well. From Figure 4, it is observed that the measured return loss at resonance is  $-15.2 \text{ dB}$ ,  $-19 \text{ dB}$ ,  $-22.3 \text{ dB}$ , &  $-27.9 \text{ dB}$ , and the measured VSWR value is 1.42, 1.25, 1.08 & 1.17 at 1.56 GHz, 2.49 GHz, 3.5 GHz, and 5.24 GHz, respectively. With reference to each resonance frequency, the proposed antenna provides impedance bandwidths of 40 MHz, 90 MHz, 100 MHz, and 90 MHz.

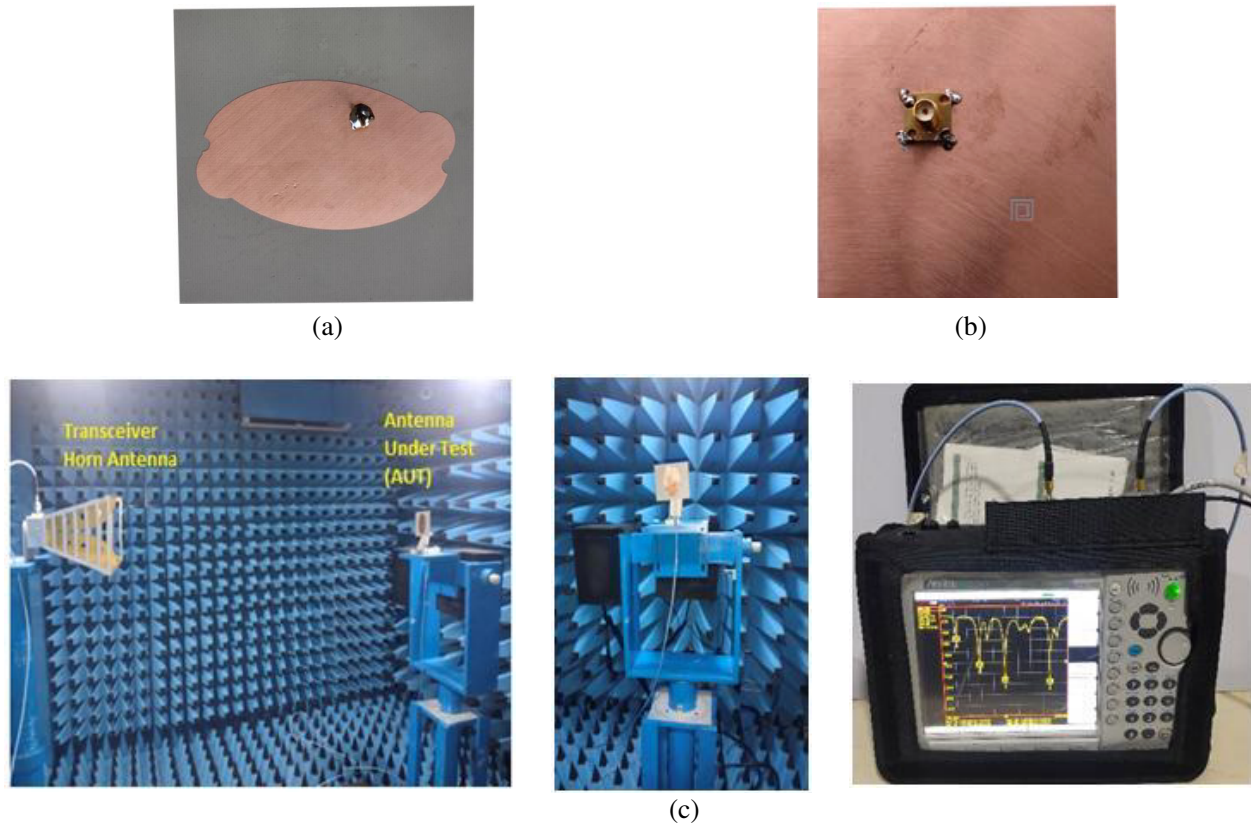
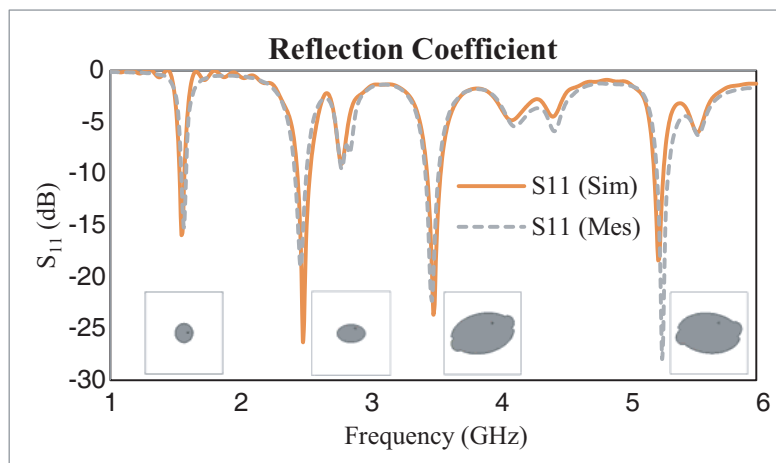


**Figure 3.** (a)–(b) Top view & bottom view of proposed fabricated antenna. (c) Photographs of measurement setup in the anechoic chamber.

The antenna is fed by coaxial probe feeding at (10 mm, 10 mm) point, and it is also tried to match the antenna’s reference impedance  $50\ \Omega$  with the line impedance of the transmitter or reception circuitry to achieve optimal power transfer as depicted in Figures 2 & 3. The feeding location is optimized using a simulation study. The simulated and measured impedances are shown in Figure 5(a) and Figure 5(b), respectively.

Figure 6 shows the current distributions at the 1.56 GHz, 2.49 GHz, 3.5 GHz, and 5.24 GHz resonance frequencies. The current concentrates at the edges of the patch by forming a loop from



(a)

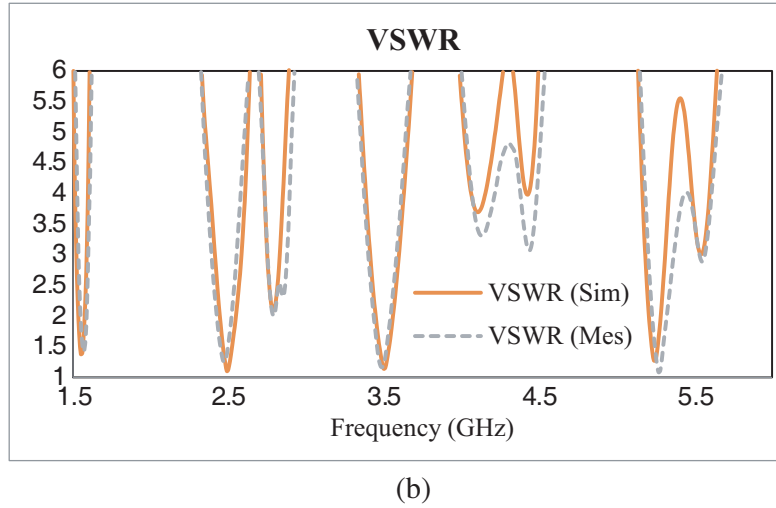


**Figure 4.** Measured and simulated (a) reflection coefficient and (b) VSWR of the proposed antenna.

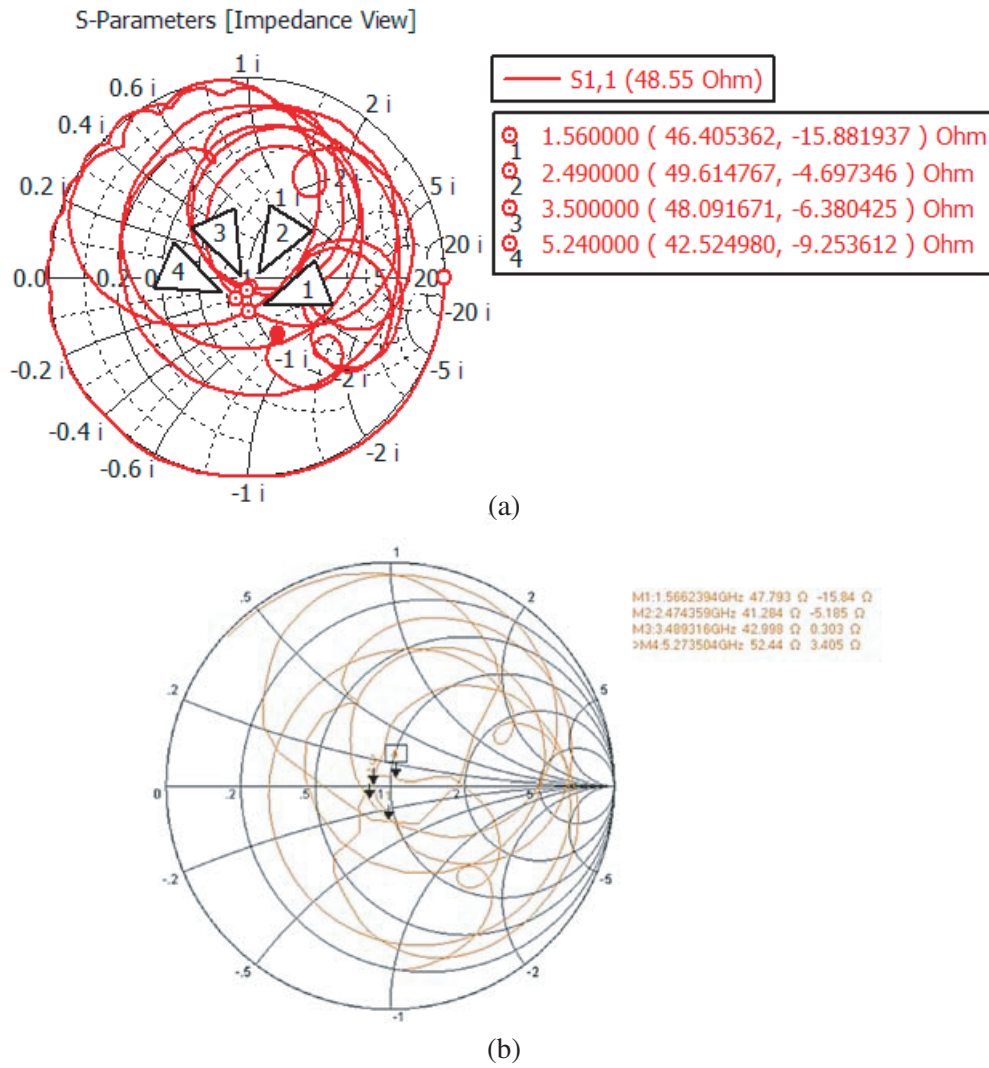


**Figure 5.** Simulated and measured impedances of the proposed antenna.

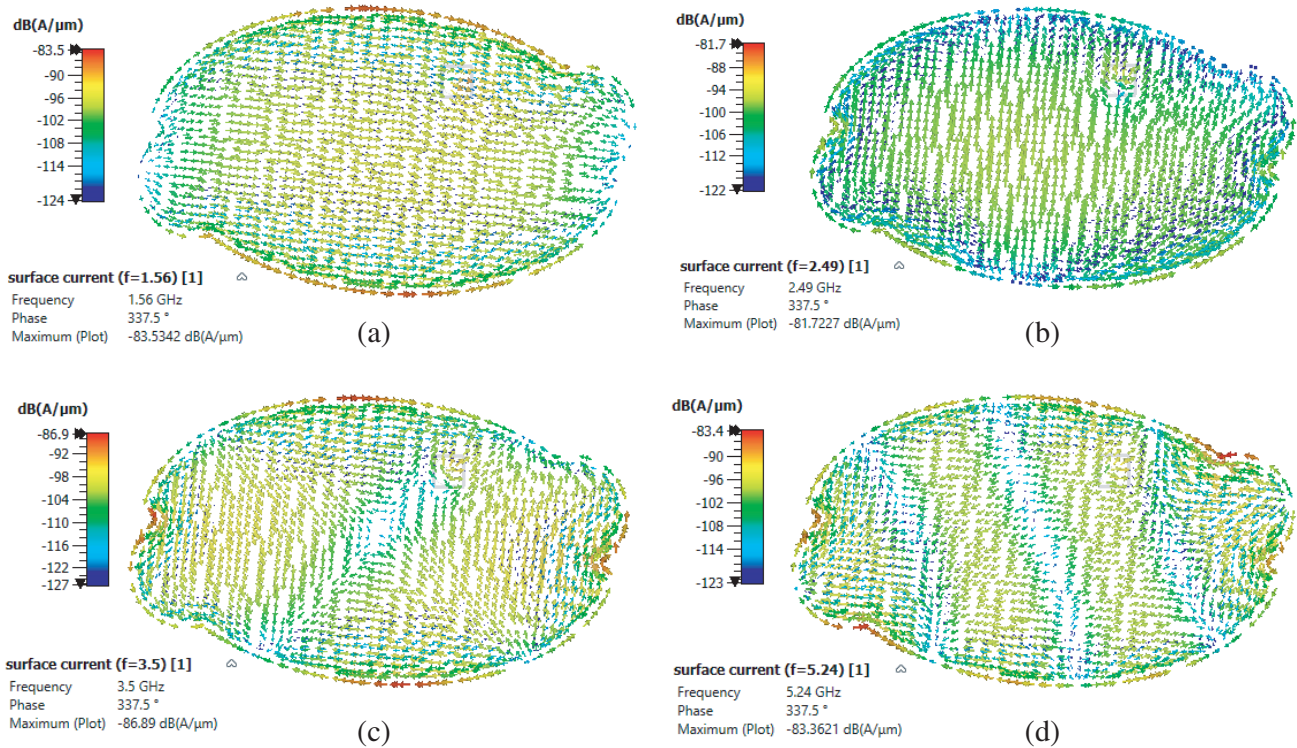
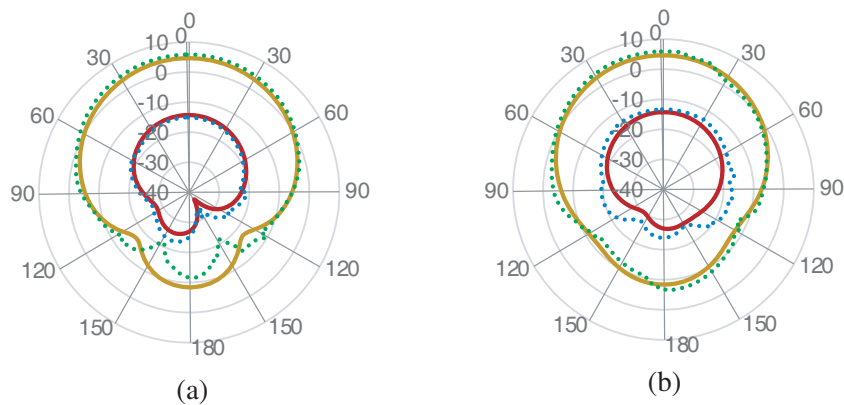


**Figure 6.** Surface current distributions at (a) 1.56 GHz, (b) 2.49 GHz, (c) 3.5 GHz and (d) 5.24 GHz of the proposed antenna.

semicircle cuts on both sides of the patch. It is also demonstrated that the current density is maximum at the center part of the patch and moves towards horizontal corners at higher frequencies. The surface current distribution at each frequency along with reshaping the antenna and changing the patch components' position also contributes to the excitation of higher-order modes and produces effective radiation at a specific band.

The simulated and measured normalized far-field radiation patterns at 1.56 GHz, 2.49 GHz, 3.5 GHz, and 5.24 GHz in *E*-plane (*yz*-plane,  $\phi = 90$ ) and *H*-plane (*xz*-plane,  $\phi = 0$ ) are shown in Figure 7. It is realized that the proposed antenna has a broadside radiation pattern at each resonant frequency, and the specific excited  $TM_{mn0}^z$  radiating modes produce a linearly polarized electric far-field in the *yz*-plane. Measured and simulated radiation patterns are matched well.

Figure 8 shows the measured radiation efficiencies of 58.7%, 94.8%, 93.2%, & 84.9% as well as measured gains of 3.49 dBi, 6.49 dBi, 4.93 dBi, & 4.46 dBi of the proposed antenna at the desired resonant frequencies. It is observed that the measured radiation efficiency and gain are matched well with the



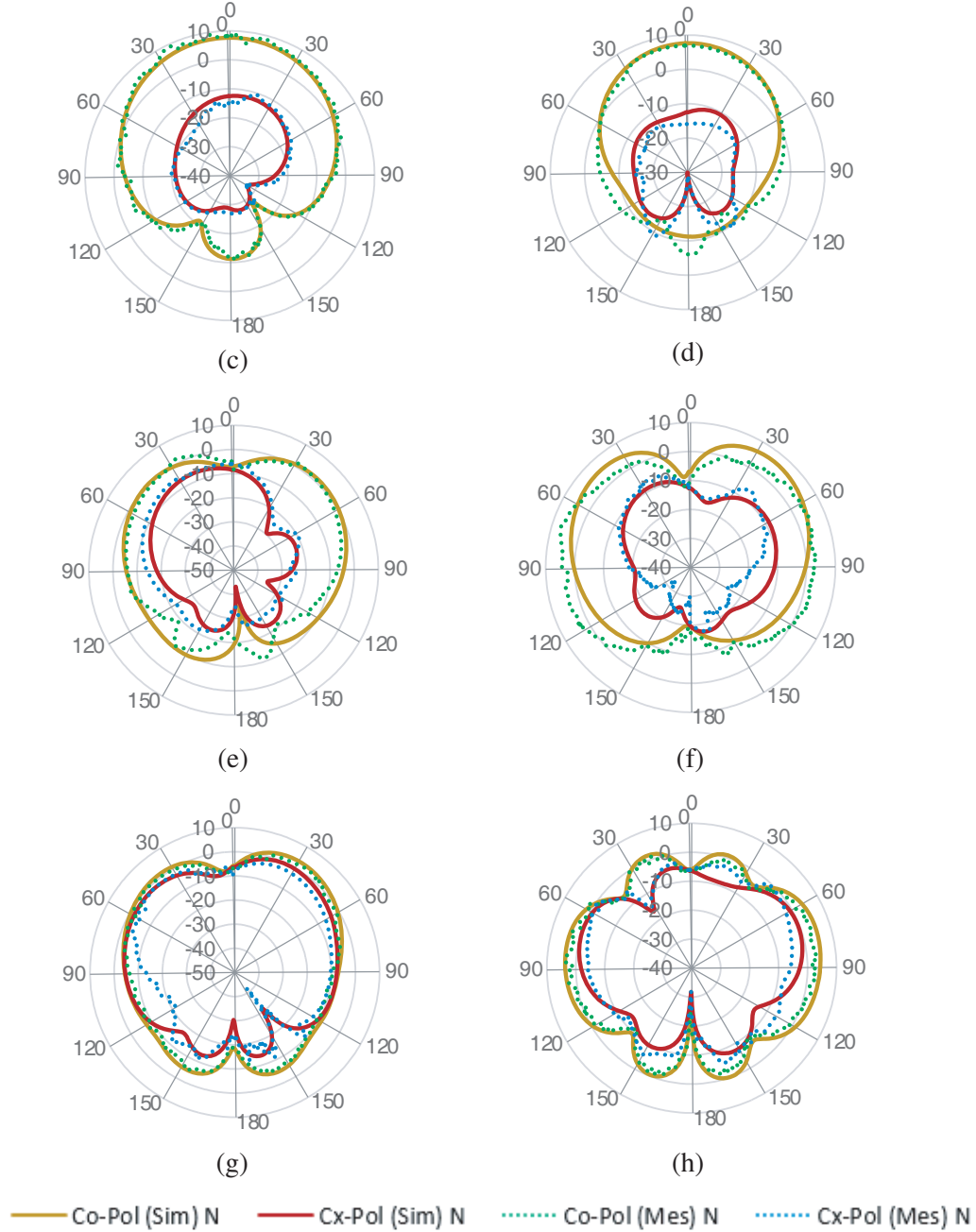


**Figure 7.** Measured and simulated normalized far-field radiation patterns of the proposed antenna: (a) E Field — 1.56 GHz, (b) H Field — 1.56 GHz, (c) E Field — 2.49 GHz, (d) H Field — 2.49 GHz, (e) E Field — 3.5 GHz, (f) H Field — 3.5 GHz, (g) E Field — 5.24 GHz, (h) H Field — 5.24 GHz.

simulated results.

Minor variations are observed between the measured and simulated results due to fabrication errors, measuring environment, and substrate characteristics. Table 1 demonstrates the performance comparison of the proposed antenna with various reported designs in terms of dimensions, geometry complexity, frequency bands, applications, methods used, substrate, gain, radiation efficiency, and feeding techniques. It is noticed that the proposed antenna offers simple, low-profile design, appropriate gain and efficiency with a similar radiation pattern to the other reported designs for the desired applications. It is observed from Table 1 that the proposed antenna is a strong contender for satellite



navigation systems along with emerging wireless communication applications used in internet of things (IoT) and 5G-enabled devices. The proposed antenna demonstrates a single layer, simple fabrication, ease of RF circuit integration, and stable radiation patterns for desired bands.

**Table 1.** Proposed antenna performance comparison with reported multi-band antennas.

Ref.	Dimension (mm <sup>3</sup> )	Frequency /Band	Application	Method Used	Substrate	Gain	Efficiency (~ %)	Feeding technique
[13]	135 × 60 × 0.5	670–1010/ 1530–2850/ 3360–3900/ 4870–8000 MHz	LTE/5G/ GPS/GSM/ UMTS/WLAN/ WiMAX	Folded driven monopole strip, Parasitic ground with slots	FR-4	0.60–4.30 dB	60.0–70.0%	Coaxial
[14]	56 × 44 × 0.8	1.575–1.665/ 2.4–2.545/ 3.27–3.97/ 5.17–5.93 GHz	GPS/WiMAX/ WLAN	Rectangular slot with a T-shaped feed patch, an inverted T-shaped stub, and E-shaped stubs	FR-4	3.55–5.02 dBi	76.8–96.6%	Microstrip
[15]	150 × 100 × 11.2	0.7–0.73/ 1.16–1.2/ 1.3–1.32/ 1.57–1.62/ 2.3–2.5/ 2.7–3.5 GHz	5G/GPS/ WLAN/ LTE/Radio Navigation	Slotted Microstrip patch	FR-4	4.30–9.00 dBi	-	Proximity & Microstrip
[16]	100 × 100 × 4.75	1.2276/1.1765/ 2.492/2.3 /2.5 GHz	IRNSS/ Satellite/ 4G/5G	Multilayer patch antenna	Rogers RT/ DUROID-5880 (tm) & FR-4	2.78 dB	-	Coaxial
[17]	120 × 120 × 29.6	1.1/1.5/ 2.3/2.6 GHz	GPS/CNSS/ WLAN/WiMAX	Dielectric Resonator	Ceramic & FR-4	5.00 dBi	-	Aperture
[18]	88.5 × 60 × 1.6	1.6/2.6/ 3.7/5.3 GHz	DCS/CDMA/ LTE/GPS/BDS/ GLONASS/ GALILEO/ WLAN/WiMAX	Monopole antenna with fractal	FR-4	1.16–3.75 dBi	40.0–72.0%	CPW
[19]	70 × 60 × 1.6	1.56/3.9/ 5.05 GHz	GPS/WLAN/ IMT	Fractal CPW Antenna	FR-4	2.25–3.06 dBi	-	CPW
[20]	73.3 × 73.3 × 4.8	1176.45/1575.42/ 2492.028 MHz	GPS/IRNSS	Stacked patch antenna	Arlon AD300N	4.69–5.39 dBi	-	Aperture
[21]	55.6 × 50.5 × 1.6	1.575/2.4/5.5/ 1.5–40 GHz	GPS/DCS/ PCS/UMTS/ ISM/IRNSS/ LTE/IoT/ Wi-MAX/ X/Ku/K/ Ka-band/ Sub-6 GHz 5G	Mushroom-shaped EBG, E-shaped decoupling structure & closed ring resonator	FR-4	7.50 dBi	-	Microstrip
This work	80 × 80 × 3.175	1.56/2.49/ 3.5/5.24 GHz	GPS/IRNSS/ Sub-6 GHz 5G/WLAN	Elliptical shape patch with narrow semicircle cut and bulges	Rogers AD 255C	3.49–6.49 dBi	58.7–94.8%	Coaxial

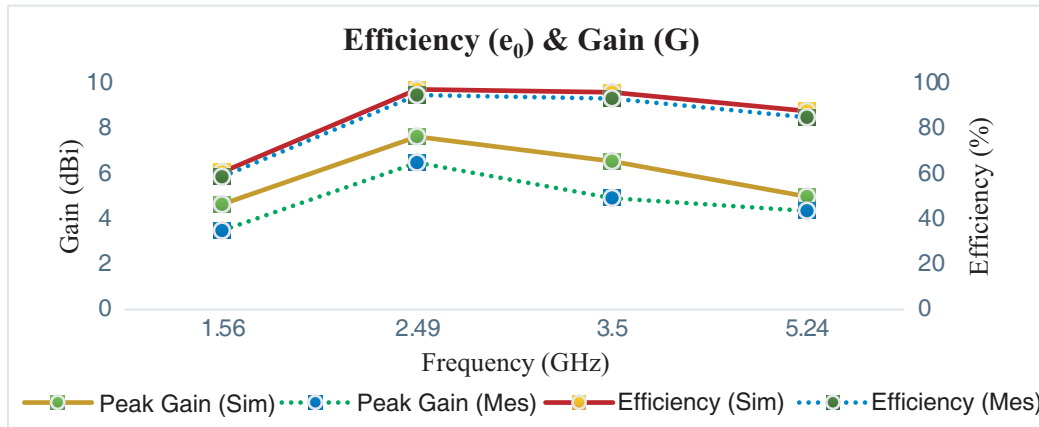


**Figure 8.** Gain and efficiency of the proposed antenna — Simulated and measured.

## 5. CONCLUSION

A multi-band antenna of an elliptical shape patch with narrow semicircle cuts and bulges on two horizontal ends resonates at 1.56 GHz, 2.49 GHz, 3.5 GHz, and 5.24 GHz is proposed for GPS, IRNSS, Sub-6 GHz 5G, and WLAN wireless applications. The proposed antenna achieves an impedance bandwidth of 40 MHz, 90 MHz, 100 MHz, and 90 MHz, peak gain of 3.49 dBi, 6.49 dBi, 4.93 dBi & 4.46 dBi, and radiation efficiency of 58.7%, 94.8%, 93.2%, & 84.9% for desired application frequencies, respectively. The antenna also offers a simple design, relatively stable and similar radiation patterns at each band. The simulated and measured results for the proposed antenna exhibit good agreement.

## ACKNOWLEDGMENT

This research is supported by STI Research Project No. GUJCOST/2020-21/1262 dated 16th September 2020 of Gujarat Council on Science and Technology (GUJCOST), Gujarat, India. We acknowledge the Electromagnetic and Antenna Research Centre (ELARC), Birla Vishwakarma Mahavidyalaya, Anand, India for using testing facilities.

## REFERENCES

1. Balanis, A., *Antenna Theory Analysis and Design*, New Jersey Wiley, Hoboken, 2016.
2. Lee, K.-F. and K.-F. Tong, "Microstrip patch antennas — Basic characteristics and some recent advances," *Proceedings of the IEEE*, Vol. 100, No. 7, 2169–2180, July 2012.
3. Patel, D. H. and G. D. Makwana, "A comprehensive review on multi-band microstrip patch antenna comprising 5G wireless communication," *International Journal of Computing and Digital Systems*, Vol. 11, No. 1, 941–953, 2022.
4. Patel, D. H. and G. D. Makwana, "Multiband antenna for 2G/3G/4G and sub-6 GHz 5G applications using characteristic mode analysis," *Progress In Electromagnetics Research M*, Vol. 115, 107–117, 2023.
5. Kumar, M. and V. Nath, "Introducing multiband and wideband microstrip patch antennas using fractal geometries: Development in last decade," *Wireless Personal Communications*, Vol. 98, No. 2, 2079–2105, 2018.
6. Ali, T., S. Pathan, and R. C. Biradar, "Multiband, frequency reconfigurable, and metamaterial antennas design techniques: Present and future research directions," *Internet Technology Letters*, Vol. 1, No. 6, e19, 2018.

7. Mruthyunjaya, L. and R. Ramasubramanian, "IRNSS signal in space ICD for standard positioning system," *Indian Space Research Organization*, 62, 2017, [http://www.isro.gov.in/irnss-programme/%0Ahttps://www.isro.gov.in/sites/default/files/irnss\\_sps\\_icd\\_version1.1-2017.pdf](http://www.isro.gov.in/irnss-programme/%0Ahttps://www.isro.gov.in/sites/default/files/irnss_sps_icd_version1.1-2017.pdf).
8. Mandal, D. and S. S. Pattnaik, "Wide CPW-fed multiband wearable monopole antenna with extended grounds for GSM/WLAN/WiMAX applications," *International Journal of Antennas and Propagation*, 1–14, 2019.
9. Kwon, O.-Y., R. Song, and B.-S. Kim, "A fully integrated shark-fin antenna for MIMO-LTE, GPS, WLAN, and WAVE applications," *IEEE Antennas and Wireless Propagation Letters*, Vol. 17, No. 4, 600–603, April 2018.
10. Naik, P., S. Ruparelia, and N. Bhatt, "Review of design strategies of dual/tri-band antennas for GPS and IRNSS applications," *ICTACT Journal on Microelectronics*, Vol. 3, No. 2, 379–384, 2017.
11. Modi, A., V. Sharma, and A. Rawat, "Compact design of multiband antenna for IRNSS, satellite, 4G and 5G applications," *2021 5th International Conference on Computing Methodologies and Communication (ICCMC)*, 6–9, Erode, India, 2021.
12. Abdullah-Al-Mamun, M., S. Datto, and M. S. Rahman, "Performance analysis of rectangular, circular and elliptical shape microstrip patch antenna using coaxial probe feed," *2017 2nd International Conference on Electrical & Electronic Engineering (ICEEE)*, 1–4, Rajshahi, Bangladesh, 2017.
13. Jalali Khalilabadi, A., "Planar multi-broadband antenna for LTE/5G/GPS/GSM/UMTS and WLAN/WiMAX wireless applications," *Wireless Personal Communications*, Vol. 118, No. 4, 2611–2620, 2021.
14. Cao, Y. F., S. W. Cheung, and T. I. Yuk, "A multiband slot antenna for GPS/WiMAX/WLAN systems," *IEEE Transactions on Antennas and Propagation*, Vol. 63, No. 3, 952–958, 2015.
15. Abdalrazik, A., A. Gomaa, and A. Kishk, "A hexaband quad-circular-polarization slotted patch antenna for 5G, GPS, WLAN, LTE, and radio navigation applications," *IEEE Antennas and Wireless Propagation Letters*, Vol. 20, No. 8, 1438–1442, 2021.
16. Modi, A., V. Sharma, and A. Rawat, "Design and analysis of multilayer patch antenna for IRNSS, GPS, Wi-Fi, satellite, and mobile networks communications," *2021 12th International Conference on Computing Communication and Networking Technologies (ICCCNT)*, 1–6, 2021.
17. Sharma, A., G. Das, S. Gupta, and R. K. Gangwar, "Quad-band quad-sense circularly polarized dielectric resonator antenna for GPS/CNSS/WLAN/WiMAX applications," *IEEE Antennas and Wireless Propagation Letters*, Vol. 19, No. 3, 403–407, 2020.
18. Yu, Z., J. Yu, X. Ran, and C. Zhu, "A novel ancient coin-like fractal multiband antenna for wireless applications," *International Journal of Antennas and Propagation*, Vol. 2017, 1–10, 2017.
19. El Nabaoui, D., A. Tajmouati, A. Errkik, L. Elabdellaoui, C. Abounaima, and M. Latrach, "Multiband fractal CPW antenna for GPS, WLAN and IMT applications," *Proceedings of the 2nd International Conference on Computing and Wireless Communication Systems*, 1–5, 2017.
20. Narayan, K. G. S., V. Velavikneshwaran, and J. A. Baskaradas, "A triband microstrip stacked patch antenna design for GPS and IRNSS applications," *2018 IEEE Indian Conference on Antennas and Propagation (InCAP)*, 1–3, Hyderabad, India, 2018.
21. Saxena, G., P. Jain, and Y. K. Awasthi, "High diversity gain super-wideband single band-notch MIMO antenna for multiple wireless applications," *IET Microwaves, Antennas & Propagation*, Vol. 14, No. 1, 109–119, 2020.
22. Trzaska, H., *EMF Measurements in the Near Field*, Nobel Publ. Co., Atlanta, USA, 2001.
23. Dlugosz, T. and H. Trzaska, "How to measure in the near field and in the far field," *Communications and Network*, Vol. 2, No. 1, 65–68, 2010.